

## Rational Introduction of Disulfide Bond to Enhance Optimal Temperature of *Lipomyces starkeyi* $\alpha$ -Dextranase Expressed in *Pichia pastoris*

Chen, Lin, Chao Yu, Xiangshan Zhou\*, and Yuanxing Zhang

State Key Laboratory of Bioreactor Engineering, East China University of Science and Technology, Shanghai 200237, China

Received: February 25, 2009 / Revised: June 23, 2009 / Accepted: July 16, 2009

$\alpha$ -Dextranase, which can hydrolyze dextran, is largely used in the sugar industry. However, a thermostable  $\alpha$ -dextranase is needed to alleviate the viscosity of syrups and clean blocked machines. Thus, to improve the optimal temperature of *Lipomyces starkeyi*  $\alpha$ -dextranase expressed by *Pichia pastoris*, the rational introduction of a *de novo* designed disulfide bond was investigated. Based on the known structure of *Penicillium minioluteum* dextranase, *L. starkeyi*  $\alpha$ -dextranase was constructed using homology modeling. Four amino acids residues were then selected for site-directed mutagenesis to cysteine. When compared with the wild-type dextranase, the mutant DexM2 (D279C/S289C) showed a more than 13°C improvement on its optimal temperature. DexM2 and DexM12 (T245C/N248C, D279C/S289C) also showed a better thermal stability than the wild-type dextranase. After the introduction of two disulfide bonds, the specific activity of DexM12 was evaluated and found to be two times higher than that of the wild-type. Moreover, DexM12 also showed the highest  $V_{\max}$ .

**Keywords:** *Lipomyces starkeyi*  $\alpha$ -dextranase, site-directed mutagenesis, *Pichia pastoris*, thermostability, disulfide bond

$\alpha$ -Dextranases (E.C. 3.2.1.11), which can hydrolyze the  $\alpha$ -1,6-glycosidic bonds in dextran polymers, are an important group of industrial enzymes [16, 17] that are playing an increasingly important role in the food, dentistry, and detergent industries. In the sugar industry, dextranases are used to lessen the viscosity of syrups and clean machines blocked by dextran [10, 15]. Furthermore, low-molecular-weight dextran produced by dextranases can be applied for clinical use [18, 35]. Some studies have even shown that dextranases can effectively block the formation of dental

plaque, which is composed of salivary glycoproteins and sticky glucose polymers [2, 23, 24].

In the particular case of the sugar industry, thermostable  $\alpha$ -dextranases are needed to lessen the syrup viscosity and clean blocked machines, as the process temperature is normally sustained at 40–50°C [10, 15]. Although the common practice to meet such a demand is to search for new thermostable dextranases from thermophilic microorganisms found in extreme environments, such as anaerobic thermophilic bacteria or *Bacillus* [13, 39], this method is limited owing to the restricted availability of thermophilic microorganisms from such special environments. Therefore, the use of a reasonable modification to create a recombinant  $\alpha$ -dextranase with an increased thermostability is more attractive for industrial applications.

Currently, directed evolution and rational design are the two main genetic strategies applied to improve the thermostability of an enzyme [6, 21, 38]. In directed evolution, mutant libraries are constructed using various methods, such as an error-prone PCR, DNA shuffling, or staggered extension process, all of which require reliable high-throughput screening for the desired mutants, which becomes a bottleneck process for this approach [37]. Meanwhile, rational design of an enzyme is mainly based on knowledge of the relationship between a protein's structure and its function. The powerfulness of rational design in altering a protein's properties has already been confirmed by many cases [5, 11, 36]. Several common features have been identified as contributing to stability, including hydrogen bonds, ion-pair interactions, hydrophobic interactions, disulfide bonds, and metal binding. Among these features, disulfide bonds are believed to stabilize proteins through an entropic effect, thereby decreasing the entropy of the protein's unfolded state [22].

Cysteine clusters are believed to preferentially form CXXC structures, and are often involved in metal coordination or disulfide bond formation. Cysteine clustering has also been shown to correlate with the growth temperature of an

\*Corresponding author

Phone: +86-21-64253306; Fax: +86-21-64253306;  
E-mail: xszhou@ecust.edu.cn

organism [30]. The stabilizing effect of disulfide bonds has already been confirmed by many mutagenesis studies involving the introduction of disulfide bonds in enzymes. For example, when Cys residues were introduced at positions Gly199 and Phe236 in subtilisin C by site-directed mutagenesis, the half-life of the mutant enzyme was 2–4.8 times longer than that of the wild-type enzyme [19]. Moreover, introducing one pair of disulfide bridges (Ser100 and Asn150) into endo- $\beta$ -1,4-xylanase (XynA) from *Bacillus stearothermophilus* No. 236 increased the thermostability of the XynA by about 5°C [14]. This improved thermal stability was also supported by an increase in the energy barrier for inactivation. Moreover, the mutation had little influence on the catalytic efficiency and other functional properties of the XynA [14]. It has also been reported that thermal unfolding detected by CD demonstrated that the formation of a disulfide bridge between A77C/G123C of a  $\beta$ -lactamase resulted in a significantly higher apparent  $T_m$  value than that of the wild-type enzyme (an increase of 7.4°C). The drug resistance of the *E. coli* mutant was also distinctively higher than that of the *E. coli* wild type [31].

In a recent study, the current authors expressed a recombinant *L. starkeyi* dextranase in *Pichia pastoris* as an active extracellular enzyme and purified it [4]. As far as is known, there has been no previous report on the modification of the disulfide bonds in a  $\alpha$ -dextranase. Accordingly, this paper presents the rational design of a recombinant *L. starkeyi*  $\alpha$ -dextranase based on a structure obtained through homology modeling using Modeller [12]. Two dextranase mutants including one pair of cysteine mutations, and one dextranase mutant including two pairs of cysteine mutations, were designed using MODIP [34]. Thereafter, the mutated *L. starkeyi* dextranases were expressed in *P. pastoris* and purified to determine the impact of the new disulfide bonds on the thermostability and biochemical properties of the dextranase.

## MATERIALS AND METHODS

### Selection of Residues for Mutations

Homology modeling was used to obtain a three-dimensional model of the dextranase through the SwissModel Web service (<http://www.expasy.org/spdbv/>), and the structures were viewed using the

Swiss-pdb viewer [12]. Only one similar model was employed, which was based on the known *Penicillium minioluteum* dextranase structures [20]. The homology of the modeled region with the *P. minioluteum* dextranase was an 85% identity. Computer programs, such as BLOCKS 14.1 (<http://blocks.fhrc.org>), MODIP, and LPC (Ligand-Protein Contacts; <http://www.weizmann.ac.il/sgedg/lpc/>) were utilized to predict the positions of the disulfide bonds. The program “design site-directed mutants” (<http://caps.ncbs.res.in/dsdbase/mainFrame.html>) was used to predict potential sites for inserting the cysteine residues [7, 9, 32, 34, 40].

### Construction of Mutants Using PCR

Using plasmid pdex-9k-His that contained the wild-type *L. starkeyi* dextranase gene [4] as the template, the dextranase gene was amplified using a PCR with the primers Dexf and Dexr (Table 1). Each of the 30 amplification cycles consisted of denaturation at 94°C for 30 s, annealing at 56°C for 30 s, and an extension at 72°C for 1 min 45 s.

An overlapping PCR was also used to produce four different site-directed mutageneses within the coding sequence of the dextranase. In DexM1, for the mutagenesis of T245 to C and N248 to C, primers DexM1f and DexM1r (Table 1) were used in the PCR experiments. In DexM2, for the substitution of D279 to C and S289 to C, primers DexM2f and DexM2r (Table 1) were used. The two disulfide bond mutations in DexM12 were constructed using DexM2 as the template. The 34 bp and 40 bp overlapping regions of the primer at positions 245, 248, 279, and 289 were designed to complement at their respective domain boundaries. Each of the 30 amplification cycles consisted of denaturation at 94°C for 30 s, annealing at 56°C for 1 min, and an extension at 72°C for 2 min. The first-round 5' and 3' end PCR products were then used for the second-round PCR without any primers, employing the following PCR program: 94°C for 30 s, 47°C for 30 s, and 72°C for 1 min 45 s (5 cycles), followed by 94°C for 30 s, 65°C for 30 s, and 72°C for 1 min 45 s (30 cycles). In the third-round PCR, the products of the second-round PCR were amplified using the primers Dexf and Dexr, generating PCR products containing the gene sequence of the mutated dextranase. The PCR program was the same as that used in the first-round PCR. The final PCR products were digested with EcoRI and NotI and then ligated into the EcoRI–NotI restriction site of pdex-9k-His to construct the expression plasmids pdexM1, pdexM2, and pdexM12 for the mutated dextranases DexM1, DexM2, and DexM12, respectively. The mutations were verified by DNA sequencing.

### Expression and Purification of Mutant Dextranase [4]

The plasmids pdexM1, pdexM2, and pdexM12 were transformed into *P. pastoris* GS115 (Invitrogen) by electroporation. The recombinants

**Table 1.** Oligonucleotide primers used for PCR in this study.

Primer	Mutation sites (amino acid)	Primer sequence
Dexf	-----	5' GCGCGAATTCATGACATTAATCTACGTG 3'
Dexr	-----	5' ATCGCGGCCGCGTTTATGGACCATTGACCC 3'
DexM1f	245/248	5' GTTCCTCATATGTGCCACACTGCACCCAGACAAT 3'
DexM1r	245/248	5' TTGTCTGGGTGCAGTGTGGGCACATATGAGGAACC 3'
DexM2f	279/289	5' CATATGATTGCAGCCGAGCTTCCCAGGGTTACCAGAGGTGCACTC 3'
DexM2r	279/289	5' ATGAACGAGTGCACCTCTGGTAACCCGGGAAGCTCGGCTGCAAT 3'

were first screened on MGY plates (YNB 1.34%, glycerol 1%, biotin  $4 \times 10^{-5}\%$ , agar 1.5%) for His<sup>+</sup>, and then on YPD-G418 plates (yeast extract 1%, peptone 2%, glucose 1%, and agar 1.5%, which contained G418 at a final concentration of 0.5, 1.0, 2.0, 3.0, and 4.0 mg/ml, respectively) in order to screen higher copies. The recombinants producing dextranase were validated further based on halo formation on MM-blue dextran T2000 plates (YNB 1.34%, biotin  $4 \times 10^{-5}\%$ , methanol 0.5%, agar 1.5%, 2% blue dextran T2000). For each mutant dextranase, the clone with the largest halo on the MM-blue dextran T2000 plates was chosen and used for further fermentation.

Thereafter, the candidate mutations were inoculated into a 5-l fermentor containing 3 l of a basic medium that consisted of 13 ml/l H<sub>3</sub>PO<sub>4</sub>, 10.6 g/l KOH, 0.82 g/l CaSO<sub>4</sub>, 18.2 g/l K<sub>2</sub>SO<sub>4</sub>, 14.9 g/l MgSO<sub>4</sub>·7H<sub>2</sub>O, 31.73 ml/l glycerol, 0.33 ml/l antifoam, and 4.5 ml/l PTM trace metal solution. The fermentation temperature, pH, and DO (dissolved oxygen) were controlled at 28°C, 6.0 (adjusted with NH<sub>3</sub>·H<sub>2</sub>O), and above 30%, respectively. When the glycerol was completely used up, as indicated by a sharp increase in the DO, methanol with 1.2% (v/v) PTM was added to induce the expression of dextranase. Here, the methanol concentration was maintained at 2% (v/v) using a methanol sensor.

Next, the active dextranase was purified using an affinity His-bind column, as previously described [4]. The fermentation broths from the 5-l fermentor were centrifuged at 8,000 ×g for 20 min at 4°C and then filtered through a 0.45-μm filter (Millipore). The supernatants were loaded onto a Ni Sepharose Fast Flow, a His-bind affinity chromatography column (Amersham Pharmacia Biotech), that was preequilibrated with buffer A (50 mM NaH<sub>2</sub>PO<sub>4</sub>, 500 mM NaCl, 20 mM imidazole, 10% glycerol, pH 6.4). The column was then re-equilibrated using buffer A and the proteins were eluted from the column with a gradient of 30% and 50% buffer B (50 mM NaH<sub>2</sub>PO<sub>4</sub>, 500 mM NaCl, 1 M imidazole, 10% glycerol, pH 6.4) at a flow rate of 2 ml/min.

#### Thiol Titration

The Cys residues were determined using Ellman's reagent under denaturing conditions [28]. The wild-type dextranase (WT) and mutated dextranases at a concentration of 2 mg/ml were denatured by boiling for 10 min in a denaturing solution containing 2% SDS, 80 mM sodium phosphate (pH 8.0), and 2 mM EDTA with or without 50 mM dithiothreitol (DTT). The denatured dextranases (reduced with DTT or nonreduced) were then concentrated using the Centricon 10 concentrator (Millipore Co.) and dialyzed against the denaturing solution to remove any DTT. The thiol reduction was carried out by mixing 30 parts of itrobenzoic acid (DTNB) with the denaturing solution for 15 min at room temperature and then measuring the absorbance at 412 nm using a molar absorbance value of 13,600 M<sup>-1</sup>·cm<sup>-1</sup>.

#### Enzymatic Activity and Kinetic Analysis

The dextranase activity was determined based on the ratio of increase in the reducing sugar concentration in a reaction with the 3,5-dinitrosalicylic acid reagent according to the method described by Miller [27]. One unit of dextranase enzyme activity was defined as the amount of enzyme that liberated the equivalent of 1 μmol of glucose in 1 min from dextran T-2000.

The kinetic rate-constant assays were performed at 30°C and pH 4.5 in three independent experiments. The dextran concentrations were varied from 0.25 to 1.5 mg. For the kinetic parameter

measurements, the initial velocity V<sub>0</sub> was determined using various substrate concentrations. The values of V<sub>max</sub> and K<sub>m</sub> were calculated using GraphPad Prism 5.00 (2007 GraphPad Software Inc). The V<sub>max</sub> values were later converted to the catalytic constant of the enzyme k<sub>cat</sub> values, and the previously determined molecular mass (67.2 kDa) of the wild-type dextranase was used for calculating k<sub>cat</sub>.

#### Optimal pH and Temperature Measurements

The effect of pH on the enzyme activity was determined by varying the pH between 3.5 and 8.5 at a temperature of 30°C. A pH of 3.5–4.5, 5.0–7.5, and 8.0–8.5 was maintained using a sodium acetate buffer (20 mM), citrate and phosphate buffer (20 mM), and sodium phosphate buffer (20 mM), respectively. The enzyme activity of each mutated and wild-type dextranase was determined between the effective temperatures of 20–60°C at their respective optimal pH.

#### Thermal Stability of Wild-Type Dextranase and Its Mutants [14]

To determine the thermal stability, the enzymes were incubated at various temperatures for 20 min, and the residual dextranase activities then assayed at 37°C and their respective optimal pH according to the method described by Miller [27].

## RESULTS AND DISCUSSION

Given the importance of dextranases in the sugar industry for alleviating the viscosity of syrups and cleaning blocked machines, much effort has been focused on screening thermostable dextranases from special environments. However, this study used rational design to optimize the properties of a dextranase and thereby its thermostability.

*L. starkeyi* dextranase and *Penicillium* dextranase were used that both belong to the glycosyl hydrolase (GH)



**Fig. 1.** Ribbon diagram of the three-dimensional structure of recombinant *L. starkeyi* dextranase DexM12, including two new disulfide bonds (indicated by arrows), based on known *Penicillium minioluteum* dextranase as template.

**Table 2.** Number of free thiol groups in the wild-type and mutant dextranases.

Dextranase	Mutation sites	[SH]/Dex molecule before DTT treatment	[SH]/Dex molecule after DTT treatment	Deduced total number of disulfide bonds
DexWT	-----	4.6	8.4	2
DexM1	T245C, N248C	4.8	10.4	3
DexM2	D279C, S289C	5.5	10.8	3
DexM12	T245C, N248C, D279C and S289C	5	13.9	4

Concentration of proteins was 2 mg/ml and the thiol titration was performed with DTNB. The total content of thiol group of each protein was deduced by subtracting the value of the oxidized protein from that of reduced protein. DexWT: wild-type dextranase.

family 49 [16]. Using the known crystal structure of the dextranase from *Penicillium minioluteum* (PDB ID: 1ogm) as the template [20], a modeled structure of *L. starkeyi* dextranase was built. Here, the constructed model of the *L. starkeyi* dextranase was divided into two domains (Fig. 1), where the first domain consisted of 200 residues, except for the 33-residue signal sequence, and the second domain included a right-handed parallel 10  $\beta$ -helical fold. The active sites formed a cavity around a 4 to 8  $\beta$ -helical fold that included Asp429, Lys349, and Asn451 within the coils, as conserved in the glycosyl hydrolase (GH) family 49. The residues Pro234 to Pro246 formed a coil that connected the first and second domains, and the coils in the second domain stabilized the  $\beta$ -helical fold.

To further confirm which sites were suitable to form disulfide bonds, a special Web site analytical tool was used. First, based on the analysis results of the program “design site-directed mutants” (<http://caps.ncbs.res.in/dsdbase//mainFrame.html>), 185 pairs of residues were identified as potential sites for a disulfide bond, and these residues fell into four categories according to their stereochemistry parameters. Category A included the positions that were best suited to form a disulfide bond in the case where the two residues were mutated into cysteine, and 13 pairs of residues did not consist of native pairs, allowing their selection for mutation (data not shown). Next, to ensure that introducing disulfide bonds would not reduce enzyme activity, the residues around the catalytic sites were excluded. Using a multiple sequence alignment, certain residues were shown to be conserved in gi|7801167\_1-616, gi|940290\_1-608, gi|88702781|gb|ABD49214.1|, and gi|3821901\_1-604 in different dextranases, along with the residues in the 4 to 8

$\beta$ -helical fold of the constructed model, indicating their potential involvement in maintaining the catalytic or substrate-binding activity. Therefore, these residues were not subjected to mutation when the mutability of the residues was determined. As previously reported, changes in these regions frequently result in a loss of activity for mutant enzymes [8]. Third, amino acid residues that appear more frequently in proteins, such as Q, S, T, and H, were also excluded, as they tend to have a negative effect on the thermal stability of a protein [3]. Thus, the final selections for the disulfide bond location to enhance the thermal stability of the enzyme were T245C/N248C and D279C/S289C, where residues 245 and 248 were chosen as they were located within the coil and connected the two domains and thus expected to stabilize the overall structure, whereas residues 279 and 289 were chosen as they connected the first and second  $\beta$ -helical in the second part and were also far away from the activity cavity. In addition, the mutants were verified by computer using Swiss-pdb viewer Spdbv 3.7 (Fig. 1).

Three plasmids, pdexM1, pdexM2, and pdexM12, containing the mutated *L. starkeyi* dextranase were constructed by site-directed mutagenesis and transformed into *P. pastoris* respectively. The recombinant strains showing the highest dextranase activity and expressing the corresponding mutated dextranase, DexM1, DexM2, or DexM12, were selected and then fermented in a 5-l fermentor. Thereafter, DexM1, DexM2, and DexM12 were purified from the supernatant and used for further characterization, as described previously [4]. The mutation sites in the dextranase are shown in Table 2. Whereas one pair of cysteine mutations was introduced into the DexM1 and DexM2 mutants, two pairs of cysteine mutations were introduced into the DexM12 mutant.

**Table 3.** Enzymatic properties of wild-type and mutant dextranases.

Dextranase	Optimal temperature (°C)	Optimal pH	Specific activity (U/mg)	$K_m$ (mg/ml)	$k_{cat}/K_m$ (U mg/ml/min)	$V_{max}$ (U/min)
DexWT	30	4.5	13.66	2.056	264	3833
DexM1	33	5.0	25.60	2.189	320	1258
DexM2	43	4.5	14.93	7.046	230	1368
DexM12	33	5.0	44.52	4.616	380	6474

Purified enzyme solutions prepared as described in Materials and Methods were used for determining optimal temperature and pH. Specific activity and the kinetic parameters of enzymatic reaction ( $K_m$  and  $k_{cat}$ ) were determined with purified enzymes as described in Materials and Methods.

### Disulfide Bond Formation in Mutants

The introduction of the newly engineered disulfide bond was verified by thiol titration of the purified wild-type dextranase and mutated dextranases, DexM1, DexM2, and DexM12, under denaturing conditions. Free thiol groups were titrated with DTNB to analyze the disulfide-bond formation in the dextranases (Table 2). The numbers of free sulfhydryl groups were obtained before and after DTT treatment, which indicated that the wild-type dextranase had two disulfide bonds. Meanwhile, DexM1 was found to have a newly introduced disulfide bond, as expected. As the wild-type enzyme had two predictable disulfide bonds at positions 44/49 and 518/522, plus four other free cysteine residues, the number of free SH groups per mutant DexM1 molecule was expected to be four in the case of the formation of a new S–S bridge, or six if no new disulfide bond formation occurred. After being treated with DTT, the number of free SH groups per molecule was estimated to be 10.4 in DexM1, 10.8 in DexM2, and 13.9 in DexM12, yet 4.8, 5.5, and 5.0, respectively, in the absence of DTT. Hence, this result confirmed the introduction of a newly engineered disulfide bond in DexM1 and DexM2, and two new disulfide bonds in DexM12.

### Effect of New Disulfide Bonds on Optimal Temperature and Thermal Stability of Dextranase

Before characterizing the enzymatic properties of the DexWT and mutant dextranases, the effect of the engineered mutation on expression was examined using an SDS-PAGE analysis. The resulting data demonstrated that the introduction of a *de novo* disulfide bond had no effect on either the protein yield or the molecular mass of the mutant dextranases at 67.2 kDa (data not shown). The optimal pH for the dextranase mutants DexM1 and DexM12 was the same at 5, compared with 4.5 for the wild-type enzyme and mutant DexM2 (Table 3, Fig. 2A).

However, as shown in Table 3 and Fig. 2B, the optimal temperature for the mutant dextranase DexM2 (D279C/S289C) was determined as 43°C. Thus, the introduction of a disulfide bond at position 279/289 greatly increased the optimal temperature by 13°C when compared with that for the wild-type enzyme. Nonetheless, there was only a slight increase in the optimal temperature, just 3°C higher than that for the wild type, when a disulfide bond was introduced at T245C/N248C (DexM1), and two disulfide bonds were introduced at T245C/N248C and D279C/S289C, respectively (DexM12).

As for the thermal stability, the DexM2 and DexM12 mutants were more stable from 50°C to 70°C when compared with the wild type (Fig. 2C). The residual activities of DexM2 were 62%, 26%, and 20%, whereas those for DexM12 were 53%, 38%, and 21% after 20 min incubation at 50°C, 60°C, and 70°C, respectively. In contrast, the residual activities of the wild-type enzyme remained at

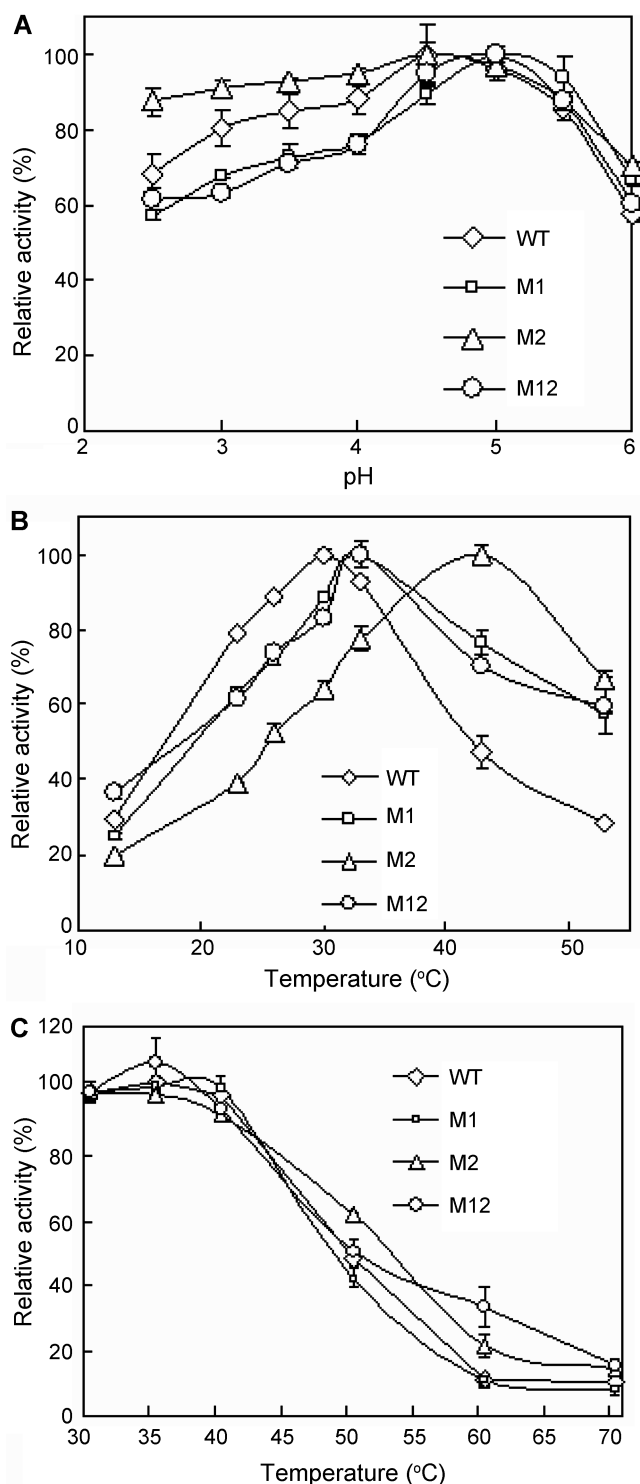


**Fig. 2.** Optimum pH (A) and temperature (B) of wild-type and mutant dextranases.

The percentage of enzyme activity was determined using the maximum activity value obtained for each enzyme sample as a reference. C. Thermostability of dextranase and mutants. The enzymes were incubated at elevated temperatures for 20 min and the residual activities then determined at 37°C and their respective optimal pH. Each temperature value is shown as the relative activity compared with that for the time-zero samples.

48%, 11%, and 10% at the corresponding temperatures, respectively. Therefore, the introduction of a disulfide bond at position 279/289 greatly increased the thermostability of the enzyme. In the case of M12, which was expected to have been more stable after introducing two disulfide bonds, the mutated residues T245C/N248C possibly had a reverse effect on the mutated residues D279C/S289C. Another reason for the improved thermostability of DexM2 may have been an increased number of hydrophobic interactions [29].

### Dextranase Enzymatic Kinetics

To study the thermodynamic details of the mutated dextranases, the steady-state kinetic parameters  $K_m$  and  $k_{cat}$  were determined. According to a Michaelis–Menten nonlinear fit, the  $K_m$  and  $V_{max}$  for DexWT, DexM1, DexM2, and DexM12 all exhibited 95% confidence intervals with a high goodness-of-fit. However, the enzymatic properties of the purified wild-type and mutant dextranases exhibited clear differences (Fig. 3). The lowest  $K_m$  was exhibited by the wild-type dextranase, as indicated by its maximal affinity to a substrate of dextran T2000, whereas the highest

$k_{cat}/K_m$  was exhibited by DexM12, indicating its high efficiency of catalysis. No distinctive difference was found between DexWT and DexM1 as regards  $K_m$ . For the hydrolysis of dextran T2000, the maximal affinity shown by DexWT and  $K_m$  was 2.056, whereas it was 7.046 for DexM2 (Table 3). The DexM12 mutant that included the two new disulfide bonds exhibited the highest  $V_{max}$ , 6,474 U/min and highest specific activity, 44.52 U/mg, which was 3.3 times higher than that of DexWT. Therefore, DexM12 was the best enzyme for catalytic efficiency. Based on the structure of the ligand BGC1575X [33], the new disulfide bonds in the mutant dextranases did not seem to be involved in the enzyme active site (data not shown). Thus, the different enzymatic properties exhibited were probably caused by a single or joint effect on the conformational flexibility of the enzyme. As such, the mutations may have resulted in less flexibility of the second domain toward the central cavity or “substrate-binding site” of the enzyme. This internal flexibility would appear to be supported by the smallest  $K_m$  for DexWT.

Consequently, when taken together, the introduction of a *de novo* disulfide bond was found to have an effect on the

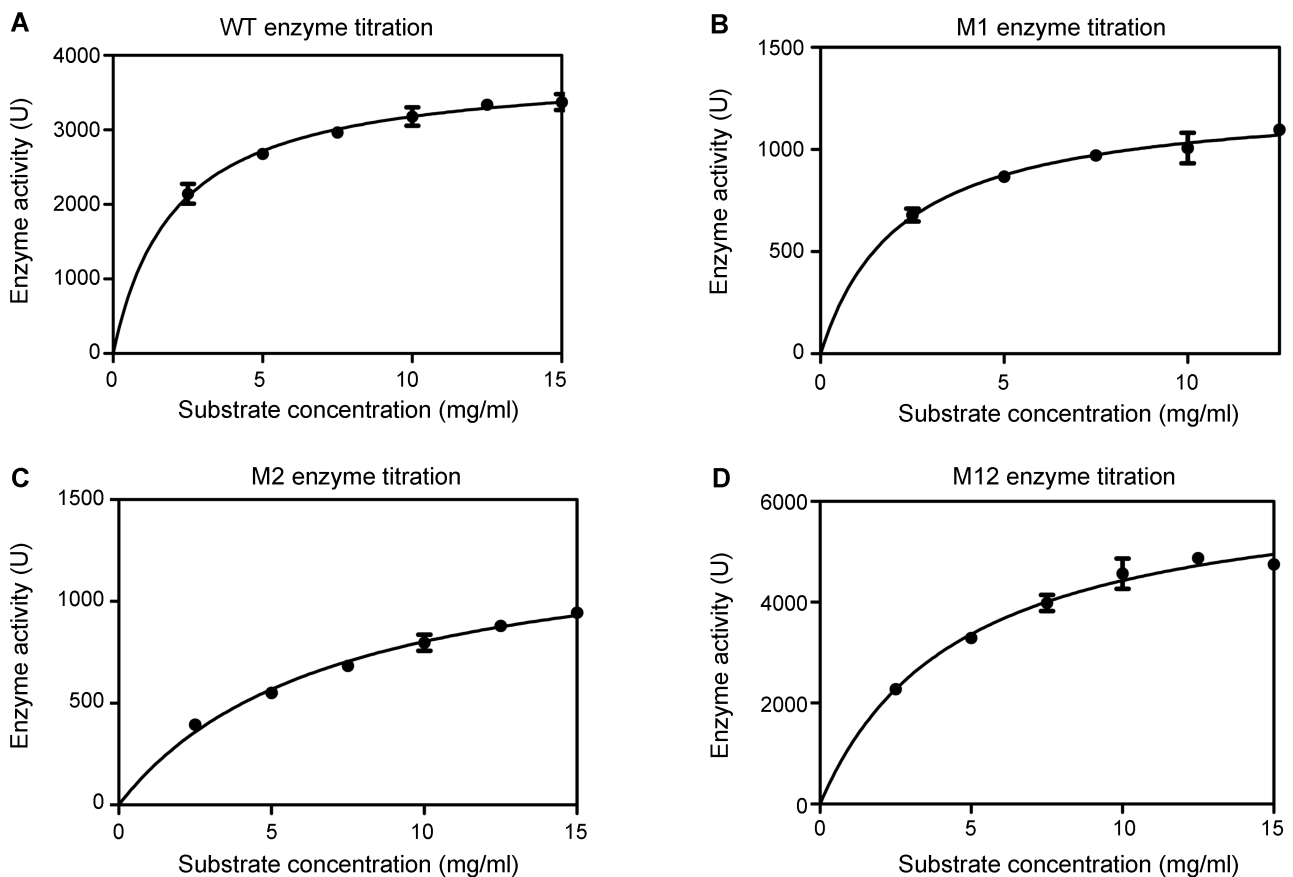


**Fig. 3.** Wild-type and mutant dextranase titrations for different substrate concentrations.

The titrations were performed at the optimal temperature and pH for each enzyme with a suitable enzyme concentration, and then fitted to the Michaelis–Menten equation using the software GraphPad Prism 5.00. The substrate was dextran T2000.

thermodynamic stability of the dextranase. The maximal optimal temperature of DexM2, including a new disulfide bond, was 13°C higher than that of the wild-type dextranase, and the thermal stability of DexM2 was also better than that of the wild-type when above 50°C, thereby proving that the induction of a disulfide bond at position 279/289 made the dextranase more stable at higher temperatures. Although M12 only showed a 3°C enhancement in its optimal temperature, it did exhibit a better thermostability. As indicated in other research, the effect of a double mutation when compared with a single mutation may be additive, partially additive, synergistic, antagonistic, or absent [25, 26]. In the present case, the mutation at sites 245/248 likely had an opposite structural effect to the mutation at sites 279/289, which increased the strain tension between the two domains. As previously reported, thermostable mutations either increase the thermodynamic stability of a protein (*i.e.*, they increase the free-energy difference between the unfolded state and the folded state) or they decrease the rate of unfolding by increasing the free-energy difference between the folded state and the transition state of unfolding [21]. In addition, there was still example that the predicted mutant enzyme was only slightly more thermostable with no CD spectroscopic changes [1].

In general, introducing disulfide bonds into proteins has been shown to facilitate folding and increase structure-based stability. Thus, the rational introduction of disulfide bonds is a more effective way of resisting thermal inactivation and can be a successful strategy for creating thermostable dextranase mutants. Accordingly, this study attempted to improve the thermostability of dextranase by rationally introducing disulfide bonds. Contrary to expectations, DexM1 did not demonstrate a significantly enhanced thermostability, whereas DexM2 displayed a surprisingly greater thermostability than DexM1 and DexM12. Whether introducing a disulfide bond at T245 and N248 destroyed the structure balance still needs to be confirmed. To meet the extremely harsh conditions encountered in industrial processes, dextranases are needed with a higher thermostability. Therefore, further studies will investigate the introduction of other modifications that have been reported to be critical factors contributing to the thermophilic nature of the glycosyl hydrolase family 49.

## REFERENCES

1. Ai, Y. C. and D. B. Wilson. 2002. Mutation and expression of N233C-D506C of cellulase Cel6B from *Thermobifida fusca* in *Escherichia coli*. *Enzyme Microb. Tech.* **30**: 804–808.
2. Banas, J. A. and M. M. Vickerman. 2003. Glucan-binding proteins of the oral streptococci. *Crit. Rev. Oral Biol. Med.* **14**: 89–99.
3. Chakravarty, S. and R. Varadarajan. 2000. Elucidation of determinants of protein stability through genome sequence analysis. *FEBS Lett.* **470**: 65–69.
4. Chen, L., X. S. Zhou, W. M. Fan, and Y. X. Zhang. 2008. Expression, purification and characterization of a recombinant *Lipomyces starkeyi* dextranase in *Pichia pastoris*. *Protein Expr. Purif.* **58**: 87–93.
5. Chen, Y., C. T. Mant, S. W. Farmer, R. E. Hancock, M. L. Vasil, and R. S. Hodges. 2005. Rational design of alpha-helical antimicrobial peptides with enhanced activities and specificity/therapeutic index. *J. Biol. Chem.* **280**: 12316–12329.
6. Chica, R. A., N. Doucet, and J. N. Pelletier. 2005. Semi-rational approaches to engineering enzyme activity: Combining the benefits of directed evolution and rational design. *Curr. Opin. Biotechnol.* **16**: 378–384.
7. Chirgadze, D. Y., J. Hepple, R. A. Byrd, R. Sowdhamini, T. L. Blundell, and E. Gherardi. 1998. Insights into the structure of hepatocyte growth factor/scatter factor (HGF/SF) and implications for receptor activation. *FEBS Lett.* **430**: 126–129.
8. Dai, M. H., E. D. Wang, Y. Xie, W. H. Jiang, and G. P. Zhao. 1999. Site-directed mutagenesis of the active center of penicillin acylase from *E. coli* ATCC 11105. *Sheng Wu Hua Xue Yu Sheng Wu Wu Li Xue Bao* (Shanghai) **31**: 558–562.
9. Donate, L. E., E. Gherardi, N. Srinivasan, R. Sowdhamini, S. Aparicio, and T. L. Blundell. 1994. Molecular evolution and domain structure of plasminogen-related growth factors (HGF/SF and HGF1/MSP). *Protein Sci.* **3**: 2378–2394.
10. Egglestona, G. and A. Monge. 2005. Optimization of sugarcane factory application of commercial dextranases. *Process Biochem.* **40**: 1881–1894.
11. Gabor, E. M. and D. B. Janssen. 2004. Increasing the synthetic performance of penicillin acylase PAS2 by structure-inspired semi-random mutagenesis. *Protein Eng. Des. Sel.* **17**: 571–579.
12. Guex, N. and M. C. Peitsch. 1997. SWISS-MODEL and the Swiss-PdbViewer: An environment for comparative protein modeling. *Electrophoresis* **18**: 2714–2723.
13. Hoster, F., R. Daniel, and G. Gottschalk. 2001. Isolation of a new *Thermoanaerobacterium thermosaccharolyticum* strain (FH1) producing a thermostable dextranase. *J. Gen. Appl. Microbiol.* **47**: 187–192.
14. Jeong, M. Y., S. Kim, C. W. Yun, Y. J. Choi, and S. G. Cho. 2007. Engineering a *de novo* internal disulfide bridge to improve the thermal stability of xylanase from *Bacillus stearothermophilus* No. 236. *J. Biotechnol.* **127**: 300–309.
15. Jiménez, E. R. 2005. The dextranase throughout the sugar-production industry. *Biotechnol. Appl.* **22**: 20–27.
16. Kang, H. K., S. H. Kim, J. Y. Park, X. J. Jin, D. K. Oh, S. S. Kang, and D. Kim. 2005. Cloning and characterization of a dextranase gene from *Lipomyces starkeyi* and its expression in *Saccharomyces cerevisiae*. *Yeast* **22**: 1239–1248.
17. Khalikova, E., P. Susi, and T. Korpela. 2005. Microbial dextran-hydrolyzing enzymes: Fundamentals and applications. *Microbiol. Mol. Biol. Rev.* **69**: 306–325.
18. Kim, D. and D. F. Day. 1994. A new process for the production of clinical dextran by mixed-culture fermentation of *Lipomyces starkeyi* and *Leuconostoc mesenteroides*. *Enzyme Microb. Tech.* **16**: 844–848.
19. Ko, J. H., W. H. Jang, E. K. Kim, H. B. Lee, K. D. Park, J. H. Chung, and O. J. Yoo. 1996. Enhancement of thermostability and catalytic efficiency of AprP, an alkaline protease from *Pseudomonas* sp., by the introduction of a disulfide bond. *Biochem. Biophys. Res. Commun.* **221**: 631–635.

20. Larsson, A. M., R. Andersson, J. Ståhlberg, L. Kenne, and T. A. Jones. 2003. Dextranase from *Penicillium minioluteum*: Reaction course, crystal structure, and product complex. *Structure* **11**: 1111–1121.
21. Lehmann, M. and M. Wyss. 2001. Engineering proteins for thermostability: The use of sequence alignments versus rational design and directed evolution. *Curr. Opin. Biotechnol.* **12**: 371–375.
22. Li, W. F., X. X. Zhou, and P. Lu. 2005. Structural features of thermozymes. *Biotechnol. Adv.* **23**: 271–281.
23. Marotta, M., A. Martino, A. D. Rosa, E. Farina, and M. Carten. 2002. Degradation of dental plaque glucans and prevention of glucan formation using commercial enzymes. *Process Biochem.* **38**: 101–108.
24. Mehvar, R. 2000. Dextrans for targeted and sustained delivery of therapeutic and imaging agents. *J. Control. Release* **69**: 1–25.
25. Mildvan, A. S., D. J. Weber, and A. Kuliopulos. 1992. Quantitative interpretations of double mutations of enzymes. *Arch. Biochem. Biophys.* **294**: 327–340.
26. Mildvan, A. S. 2004. Inverse thinking about double mutants of enzymes. *Biochemistry* **43**: 14517–14520.
27. Miller, G. L. 1959. Use of dinitrosalicylic acid reagent for the determination of reducing sugars. *J. Anal. Chem.* **31**: 426–428.
28. Robyt, J. F., R. J. Ackerman, and C. G. Chittenden. 1971. Reaction of protein disulfide groups with Ellman's reagent: A case study of the number of sulfhydryl and disulfide groups in *Aspergillus oryzae* -amylase, papain, and lysozyme. *Arch. Biochem. Biophys.* **147**: 262–269.
29. Rodriguez, E., Z. A. Wood, P. A. Karplus, and X. G. Lei. 2000. Site-directed mutagenesis improves catalytic efficiency and thermostability of *Escherichia coli* pH 2.5 acid phosphatase/phytase expressed in *Pichia pastoris*. *Arch. Biochem. Biophys.* **382**: 105–112.
30. Rosato, V., N. Pucello, and G. Giuliano. 2002. Evidence for cysteine clustering in thermophilic proteomes. *Trends Genet.* **18**: 278–281.
31. Shimizu-Ibuka, A., H. Matsuzawa, and H. Sakai. 2006. Effect of disulfide-bond introduction on the activity and stability of the extended-spectrum class A  $\beta$ -lactamase Toho-1. *Biochim. Biophys. Acta* **1764**: 1349–1355.
32. Srinivasan, N., R. Sowdhamini, C. Ramakrishnan, and P. Balam. 1990. Conformations of disulfide bridges in proteins. *Int. J. Pept. Protein Res.* **36**: 147–155.
33. Sobolev, V., A. Sorokine, J. Prilusky, E. E. Abola, and M. Edelman. 1999. Automated analysis of interatomic contacts in proteins. *Bioinformatics* **15**: 327–332.
34. Sowdhamini, R., N. Srinivasan, B. Shoichet, D. V. Santi, C. Ramakrishnan, and P. Balam. 1989. Stereochemical modeling of disulfide bridges. Criteria for introduction into proteins by site-directed mutagenesis. *Protein Eng.* **3**: 95–103.
35. Thoren, L. 1981. The dextrans – clinical data. *Devel. Biol. Stand.* **48**: 157–167.
36. Tindbaek, N., A. Svendsen, P. R. Oestergaard, and H. Draborg. 2004. Engineering a substrate-specific cold-adapted subtilisin. *Protein Eng. Des. Sel.* **17**: 149–156.
37. Turner, N. J. 2003. Directed evolution of enzymes for applied biocatalysis. *Trends Biotechnol.* **21**: 474–478.
38. Williams, G. J., A. S. Nelson, and A. Berry. 2004. Directed evolution of enzymes for biocatalysis and the life sciences. *Cell Mol. Life Sci.* **61**: 3034–3046.
39. Wynter, C. V. A., M. Chang, and J. De Jersey. 1997. Isolation and characterization of a thermostable dextranase. *Enzyme Microb. Technol.* **20**: 242–247.
40. Zhou, H., M. J. Mazzulla, J. D. Kaufman, S. J. Stahl, P. T. Wingfield, J. S. Rubin, D. P. Bottaro, and R. A. Byrd. 1998. The solution structure of the N-terminal domain of hepatocyte growth factor reveals a potential heparin-binding site. *Structure* **6**: 109–116.